Effect of cell arrangement and interstitial volume fraction on the diffusivity of monoclonal antibodies in tissue

Ardith W. El-Kareh, Samuel L. Braunstein, and Timothy W. Secomb
Department of Physiology, University of Arizona, Tucson Arizona 85724 USA

ABSTRACT We present theoretical calculations relating the effective diffusivity of monoclonal antibodies in tissue (D_{eff}) to the actual diffusivity in the interstitium (D_{int}) and the interstitial volume fraction ϕ. Measured diffusivity values are effective values, deduced from concentration profiles with the tissue treated as a continuum. By using homogenization theory, the ratio D_{eff}/D_{int} is calculated for a range of interstitial volume fractions from 10 to 65%. It is assumed that only diffusion in the interstitial spaces between cells contributes to the effective diffusivity. The geometries considered have cuboidal cells arranged periodically, with uniform gaps between cells. D_{eff}/D_{int} is found to generally be between $(^2/_3)\phi$ and ϕ for these geometries. In general, the pathways for diffusion between cells are not straight. The effect of winding pathways on D_{eff}/D_{int} is examined by varying the arrangement of the cells, and found to be slight. Also, the estimates of D_{eff}/D_{int} are shown to be insensitive to typical nonuniformities in the widths of gaps between cells.

From our calculations and from published experimental measurements of the effective diffusivity of an IgG polyclonal antibody both in water and in tumor tissue, we deduce that the diffusivity of this molecule in the interstitium is one-tenth to one-twentieth its diffusivity in water. We also conclude that exclusion of molecules from cells (an effect independent of molecular weight) contributes as much as interstitial hindrance to the reduction of effective diffusivity, for small interstitial volume fractions (around 20%). This suggests that the increase in the rate of delivery to tissues resulting from the use of smaller molecular-weight molecules (such as antibody fragments or bifunctional antibodies) may be less than expected.

INTRODUCTION

It has recently been recognized (1) that one of the major limitations to the use of monoclonal antibodies in cancer therapy is the great difficulty in delivering them inside tumors of centimeter or larger size on a reasonable time scale. This difficulty is due to the small diffusivity of the antibody molecules, and the fact that diffusion through the interstitium is the main mechanism of transport, since the vasculature inside the tumor is frequently nonfunctional. While monoclonal antibodies can be actively internalized by cells after binding to their surface, there is no significant *diffusive* flux of molecules through the cell membranes. Instead, molecules diffuse along the tortuous interstitial spaces between cells, with some diffusivity D_{int}. Because a typical antibody molecule has molecular weight around 150,000, the rate of diffusion is very slow.

The only experimental methods currently available for measuring diffusivities of molecules in tissue are indirect: the diffusivity is deduced from concentration profiles (2), or by the FRAP (fluorescence recovery after photobleaching) technique (3). Since neither the concentration nor the fluorescence intensity can be resolved on length scales comparable to cell diameters, these methods do not measure D_{int}. Instead, they measure the *effective* diffusivity D_{eff}, meaning the diffusivity in the tissue seen as a continuum, that is, averaged over many cells. The time scale for delivery of a macromolecule such as a monoclonal antibody to the center of a tumor will be inversely proportional to D_{eff}.

D_{eff} is significantly lower than the diffusivity in water, D_{aq}, for two main reasons: (*a*) volume exclusion: monoclonal antibodies are excluded from the volume occupied by the cells, and (*b*) interstitial structure: the interstitium has a structure of fibers and gel that hinders the transport of large molecules (reference 4). This can be written as:

$$D_{eff} = \underbrace{\left(\frac{D_{eff}}{D_{int}}\right)}_{\text{volume exclusion}} \underbrace{\left(\frac{D_{int}}{D_{aq}}\right)}_{\text{interstitial structure}} D_{aq}. \qquad (1)$$

The first factor D_{eff}/D_{int} is independent of molecular weight, and depends on the volume fraction ϕ of the interstitium, and the geometry of the cell arrangement. The second factor D_{int}/D_{aq} is independent of ϕ, if it can be assumed that antibodies diffuse mostly in the bulk of the interstitium, unaffected by cell membranes. This assumption is justified if the typical gap width between cells, around half a micron, is much larger than the radius of a monoclonal antibody. The Stokes–Einstein radius of albumin (molecular weight 67,000) is 0.0036 μm (5). Scaling this up to molecular weight 150,000 (for a typical IgG monoclonal antibody) gives a rough estimate of 0.005 μm for molecular radius, which is much less than 0.5 μm.

Currently available experimental techniques cannot quantify the relative magnitudes of the volume exclu-

Address correspondence to Dr. Ardith W. El-Kareh, Department of Physiology, Arizona Health Sciences Center, University of Arizona, Tucson, Arizona 85724, USA.

0006-3495/93/05/1638/09 $2.00

sion and interstitial structure effects. Therefore, it is useful to develop theoretical models to quantify the volume exclusion effect. In this paper, for several representative geometries of cells, D_{eff}/D_{int} is calculated theoretically as a function of ϕ. The sensitivity of D_{eff}/D_{int} to the geometry is examined. From these results, conclusions are drawn regarding the relative contributions of interstitial structure and exclusion from cells to the hindrance of diffusion. The results allow estimation of diffusivities in tissues with any value of interstitial volume fraction ϕ, once diffusivity as a function of molecular weight is known for one particular value of ϕ, assuming that the interstitial structure of different tissues hinders diffusion to approximately the same extent.

There has been much previous work on obstructed diffusion, as reviewed by Torquato (6, 7). Much of the work concerns diffusion obstructed by regions occupied by non-intersecting or intersecting spheres, in ordered or random arrangements. This work has limited applicability to the modeling of biological cells, for reasons now discussed. The closest packing of non-intersecting spheres gives an interstitial volume fraction of 0.2595 (p. 417 of reference 8), and random packing of spheres gives ϕ in the range 0.38–0.47, whereas measured values of ϕ as low as 0.13 have been reported for some tumors (9).

Lower interstitial volume fractions may be achieved by representing the excluded region by overlapping spheres. However, the resulting interstitial geometry is very different to that observed. (See, for example, autoradiographs of ovarian tumor xenografts from mice in Fig. 6 of reference 10, and photomicrographs of breast carcinoma tissue sections in Fig. 2 of reference 11.) For small values of ϕ, this model results in many overlaps between neighboring spheres, with no continuous interstitial region between them. In contrast, sections through cells generally show each cell to be surrounded by a continuous interstitial region. The overlapping sphere model predicts "dead ends" and completely disconnected regions of interstitial space, features rarely if ever observed in tissue sections. Therefore, neither non-overlapping spheres nor overlapping spheres provides a good representation of observed cell geometries.

The assumption that cell shapes are approximately polyhedral, rather than spherical, is more consistent with observed arrangements of cells in tissue, especially when ϕ is small. In fact, if cell shapes are assumed to be convex, then they are necessarily polyhedral in the space-filling limit $\phi \to 0$. Several experimental studies on the three-dimensional arrangement of cells and the packing of other convex, deformable particles have shown that their typical shapes are polyhedral, with an average of 14 faces. Each face corresponds to a neighboring particle or cell. The 14-sided shape (or tetrakaidecahedron) was described by Kelvin (12) in the context of bubble shapes. Examples of plant and animal cells are cited by Matzke (Table 8 of reference 13). Kittrell et al. (14) noted some

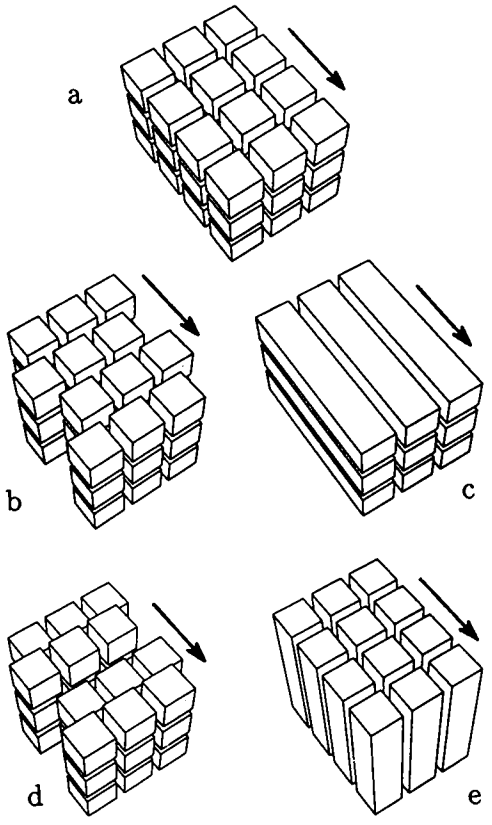

FIGURE 1 The idealized cell configurations modeled in this paper. (Arrows show direction of diffusion.)

"cuboidal" cell shapes in light micrographs of cultured normal epithelial cells, and described all their cultures as containing "cells that are polygonal to angular in shape."

For our model, we have chosen cuboidal cells because they have the simplest possible polyhedral shape (Fig. 1). These cells are arranged in ordered periodic arrays. With this configuration, the complete range of values of ϕ can be realized. Moreover, the 14-neighbor condition can be achieved with a periodic staggered arrangement of cuboids, in which two opposite faces each have four neighboring cells, two opposite faces each have two neighboring cells, and the remaining two faces each have one neighbor. While the cuboidal geometry does not reproduce actual cell shapes, it permits investigation of the effects on effective diffusivity of two key factors: interstitial volume fraction, and the way in which the cells are packed together (aligned or staggered). These are considered key factors for the following reasons. The fraction of interstitial space is clearly important because it indicates how much room there is for molecules to move in. If the cells are typically arranged in a staggered fashion, molecules will generally have to travel longer pathways than they would if the cells are aligned (Fig. 2). For this reason, staggered cell arrangements are expected to result in lower effective diffusivities than aligned arrangements.

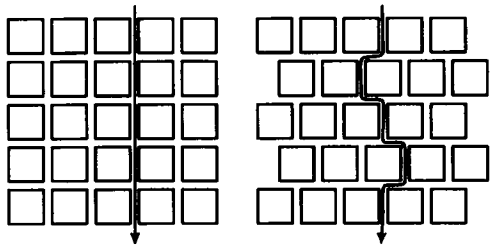

FIGURE 2 Molecules diffusing around staggered cells travel longer distances than molecules diffusing around aligned cells.

An understanding of the relative importance of interstitial structure and volume exclusion has implications for the improvement that can be expected upon using antibody fragments (1, 15) instead of whole antibody. It is generally assumed that fragments will diffuse faster in tissue because they are smaller, but predicting this improved diffusion rate is not straightforward. The diffusivity of a large nonpolar molecule in *water* is determined mainly by its molecular weight; it correlates well with molecular weight to some negative power (as can be seen from the Stokes–Einstein relation). However, in *tissue*, the diffusivity depends also on ϕ, because of the volume exclusion effect. Since dosimetry estimates depend crucially on the amount of uptake of antibody (16), which in turn has a strong dependence on diffusion time scales (1), an understanding of how diffusivity varies with other variables besides molecular weight is important.

MODEL

To quantify the volume exclusion effect, we use a theoretical model to compute the ratio $D_{\text{eff}}/D_{\text{int}}$ for several idealized geometric arrangements of cuboidal cells (Fig. 1). The first three configurations involve periodic arrangement of cubic cells (i.e., side lengths in the proportion 1:1:1), and are chosen to investigate the effect of staggering, by having the cells (*a*) aligned, (*b*) staggered in one direction, and (*c*) staggered in two directions. The two further configurations are chosen to investigate the effect of cell elongation, by having the cells (*a*) aligned and cubic (1:1:1) as before, (*d*) elongated (5:1:1) in the direction of diffusion, and (*e*) elongated (1:5:1) in a direction perpendicular to diffusion. The interstitial spaces between cells are the same width in all directions. This width is varied relative to the cell size to give a range of interstitial volume fractions. Note that the ratio $D_{\text{eff}}/D_{\text{int}}$ does not depend on the absolute cell dimensions, only on the relative dimensions of cells and interstitial spaces.

It is assumed that antibodies cannot permeate inside the cells. No assumption about binding to cell surfaces is made, since binding gives rise to an effective reaction rate but does not change the effective diffusivity (as shown below). A final assumption is that the average concentration of antibody varies over length scales large compared to cell size. This holds easily even for millimeter-sized micrometastases.

PRELIMINARY ESTIMATES OF D_{eff}

The factor $D_{\text{eff}}/D_{\text{int}}$ is related to tortuosity, which has been defined in several ways by different authors, for media where diffusion occurs only in the void fraction (with D_{int} being the diffusivity in the void). Bear (17), in a discussion of diffusion in porous media, defines tortuosity as $\tau \equiv D_{\text{eff}}/D_{\text{int}}$. Schultz and Armstrong (18), in their study of muscle permeability, define tortuosity as $\tau \equiv \phi D_{\text{int}}/D_{\text{eff}}$. Nicholson and Phillips (19), in their work on diffusion of ions in the brain, use the definition $\tau = \sqrt{D_{\text{int}}/D_{\text{eff}}}$, with the square root appearing because of their interpretation of τ in terms of path length.

While bounds for tortuosity of media with spherical and cylindrical obstacles, and for random media, are given in the literature (7), the case of cuboidal obstacles does not appear to have been considered. In three dimensions, for diffusion occurring with constant diffusivity D_{int} in only a fraction ϕ of the medium, and in the absence of any further information on geometric structure,

$$0 \le \frac{D_{\text{eff}}}{D_{\text{int}}} \le \phi \tag{2}$$

(per reference 7). The upper bound (of maximally efficient diffusion) is attained when all the interstitial volume consists of straight channels of uniform width running along the direction of diffusion. In this case, the tortuosity $\tau = 1$, using the definition of Schultz and Armstrong (18). For our model of ordered cuboidal cells, an example is the case of cuboidal cells aligned and extremely long in the direction of diffusion (so that a negligible fraction of the interstitial volume consists of channels perpendicular to the diffusion direction). This limit is also approached if the spacings between cell faces perpendicular to the diffusion direction are much smaller than the spacings between other cell faces.

Normally, however, biological cells are not very elongated, and the spacings between them are about the same in all directions. Thus, the upper bound in (2) is not achieved, and the tortuosity $\tau \ge 1$, again using the definition of Schultz and Armstrong (18). For an isotropic medium, the upper bound

$$\frac{D_{\text{eff}}}{D_{\text{int}}} \le \frac{2\phi}{3 - \phi} \tag{3}$$

has been given by Milton (20). For the aligned cubic case, a lower bound can also be obtained. In this case, the molecules diffuse along channels parallel to the net flux, which connect with side channels (the spaces between cell faces normal to the direction of net flux). If mole-

cules were excluded from these side channels, the remaining channels would have uniform width and would occupy slightly more than two-thirds of the interstitial volume, and so D_{eff}/D_{int} would be bounded below by $2\phi/3$. Including the side channels can only increase the effective diffusivity, and so $2\phi/3$ is a lower bound for the aligned cubic case. (The fact that adding side branches to a channel increases the flux through it, for a given imposed concentration difference, can be proved by a simple argument using the well-known Dirichlet integral (21), which is minimized for solutions of the diffusion equation.)

For aligned cubic cells in an isotropic array, then,

$$\frac{2}{3}\phi \le \frac{D_{eff}}{D_{int}} \le \frac{2\phi}{3-\phi}. \tag{4}$$

Actual arrangements of cells may differ from this idealized case in three main respects: (*a*) the cells may not be aligned in rows; (*b*) the cells or the gaps may be widened preferentially in one particular direction, leading to an anisotropic arrangement; and, (*c*) typical cell shapes are not regular, and so gap widths are non-uniform. The effects of non-aligned and anisotropic arrangements are analyzed below. First, however, the effects of non-uniform gap widths are considered.

How sensitive is the effective diffusivity to channel width variations? First, we consider the limiting case of variations of arbitrary amplitude but with length scales much larger than the channel width. In this "long-wavelength" limit, the diffusion is nearly one-dimensional. Suppose each channel has periodically varying cross-sectional area $A(x)$ and average area A_{avg}, and that the channels occupy a volume fraction ϕ. Then the diffusive flux along each channel is independent of x and is given by:

$$J = -DA(x)\frac{dc}{dx}, \tag{5}$$

where c is the concentration and D is the diffusivity within the channel. This may be rearranged and integrated to give

$$c(0) - c(L) = \frac{J}{D}\int_0^L \frac{1}{A(x)}\,dx, \tag{6}$$

where L is the period of the variations. The effective diffusivity D_{eff} is defined as the ratio of flux per unit tissue area ($\phi J/A_{avg}$ in this case) to average concentration gradient, which gives

$$D_{eff} \equiv \frac{\phi J/A_{avg}}{[c(0)-c(L)]/L} = \frac{\phi DL}{A_{avg}}\left[\int_0^L \frac{1}{A(x)}\,dx\right]^{-1}. \tag{7}$$

For fixed ϕ and D, D_{eff} has its maximum value of ϕD when $A(x)$ is constant along the channels.

Consider now a channel of sinusoidally varying width,

$$A(x) = A_{avg}\left[1 + \alpha \sin\left(\frac{2\pi x}{L}\right)\right]. \tag{8}$$

From the above formula,

$$D_{eff} = D\phi\sqrt{1-\alpha^2}. \tag{9}$$

Even for $\alpha = 0.5$, where the range of channel widths is quite large, from $0.5A_{avg}$ to $1.5A_{avg}$, this gives $D_{eff} = 0.87\phi D$, which is not very far from the result for constant channel area. If the wavelength of the variations is not very long, the diffusion will be two-dimensional, and the validity of the long-wavelength approximation is questionable. However, in the Appendix, we justify the long-wavelength approximation, for wavelengths comparable to channel width, by comparison with an exact result. The conclusion is that effective diffusivity may be influenced by average cross-sectional areas of interstitial channels, and orientation of these channels relative to the concentration gradient, but deviations in channel width from the average are not a very important factor.

CALCULATION OF EFFECTIVE DIFFUSIVITY

This section describes the estimation of effective diffusivity for periodic arrays of cuboidal cells. The effective diffusivity is defined by

$$\mathbf{J} = -\mathbf{D}_{eff}\cdot\nabla\langle c\rangle \tag{10}$$

where $\mathbf{J}$ denotes the flux, and $\langle c\rangle$ is the average concentration of free molecules (i.e., those not bound to cell surfaces or other structures). Therefore the effective diffusivity depends on the definition of the average $\langle\ \rangle$. The purpose of averaging is to avoid considering detailed variations on the cellular length scale, or, what is nearly the same, L_c, the length of a single periodic unit (depending on the geometry, a periodic unit will not always contain exactly one cell). Averages are therefore taken over some number N of periodic units, with $N \gg 1$, but the average concentration should not depend on the exact choice of N, as long as N is sufficiently large. Moreover, the effective diffusivity is useful only if it does not depend on $\langle c\rangle$. Both these requirements necessitate that, on the length scale NL_c, the concentration must be the superposition of a linear function of position and a periodic one with period L_c. In general, this is a good approximation as long as N is not chosen too large, that is, $NL_c \ll L_t$, where L_t is the tissue length scale. Since L_c is in microns and L_t is in millimeters to centimeters or more, a range of N satisfying $1 \ll N \ll 1/\epsilon$, where $\epsilon \equiv L_c/L_t$, exists in practice.

The method used has been developed formally as homogenization theory (22), but the essential point is the representation of the concentration as the sum of a linear function of position, and a function that is periodic with period L_c. In the analysis that follows, the periodic func-

tion corresponding to an overall unit negative concentration gradient in the jth coordinate direction is represented by $\chi^j (j = 1, 2, 3)$. For the geometries considered here, χ^j is computed numerically. An imposed concentration gradient of -1 in the x_j direction gives a local concentration gradient of $-\mathbf{e}_j + \nabla\chi^j$, and this is multiplied by the local diffusivity and averaged over a unit cell to give the resulting flux, from which the effective diffusivity in the x_1 direction is deduced.

The procedure is now presented with the more formal multiple-scale approach of Bensoussan et al. (22). Two Cartesian coordinate systems are used: $\mathbf{x} = (x_1, x_2, x_3)$, on the tissue length scale L_t, and $\mathbf{y} = (y_1, y_2, y_3) = \mathbf{x}/\epsilon$ on the cellular length scale L_c. Because antibodies diffuse around cells, but not through them, the local diffusivity may be considered to be a function of position; it is zero inside the cells and equal to D_{int} in the interstitium. That is, the transport of molecules through tissue is governed by the diffusion equation with a diffusivity that varies on length scales comparable to cell sizes:

$$\frac{\partial c}{\partial t} = \frac{\partial}{\partial x_1}\left(D(\mathbf{y})\frac{\partial c}{\partial x_1}\right) + \frac{\partial}{\partial x_2}\left(D(\mathbf{y})\frac{\partial c}{\partial x_2}\right) + \frac{\partial}{\partial x_3}\left(D(\mathbf{y})\frac{\partial c}{\partial x_3}\right) + r(c, \mathbf{y}). \quad (11)$$

This equation includes the assumption, justified earlier, that diffusion in the interstitium can be modeled by continuum equations. It is also assumed that the interstitium is isotropic, since no evidence has been given for interstitial fibers being preferentially aligned parallel or perpendicular to interstitial channels. The final term on the right of Eq. 11 allows for binding to the cell surfaces with a rate that is some function of concentration. If, as is often the case, the binding sites are far from saturation, first-order kinetics is probably appropriate. On the other hand, some researchers (23) have presented evidence that predosing with unlabeled antibody to saturate binding sites in the outer regions of the tissue may improve total uptake; in this case the kinetics may be in the nonlinear regime. However, this reaction term may be nonlinear in c without affecting the following. For the periodic model cell arrangements chosen above, the functions D and r are periodic in $\mathbf{y}$.

To obtain an equation convenient for predicting concentration profiles on the tissue length scale L_t, Eq. 11, is averaged or "homogenized" on the length scale NL_c. Bensoussan et al. (22) show that, in the limit $\epsilon \to 0$, the homogenized version of Eq. 11 is

$$\frac{\partial\langle c\rangle}{\partial t} - \left[\frac{1}{V}\int_P \left(D(\mathbf{y})\delta_{ij} - D(\mathbf{y})\delta_{ik}\frac{\partial\chi^j}{\partial y_k}\right)d\mathbf{y}\right]\frac{\partial^2\langle c\rangle}{\partial x_i \partial x_j} + \frac{1}{V}\left(\int_P r(\langle c\rangle, \mathbf{y})\,d\mathbf{y}\right) = 0, \quad (12)$$

where $\langle c\rangle$ is the average concentration, V is the volume of a single periodic unit P, and δ_{ij} is the Kronecker delta. The homogenization of the diffusion operator is given by Bensoussan et al.'s equation (reference 22, Eq. 2.20, p. 16); the generalization to include the time derivative can be found in their (reference 22, Eq. 1.44, p. 242); and the homogenization of the reaction term in the nonlinear case is shown in their (reference 22, Eq. 16.12, p. 202). Bensoussan et al. show that χ^j, the periodic component of the concentration c, must be solved for from the equation

$$\frac{\partial}{\partial y_i}\left[D(\mathbf{y})\frac{\partial\chi^j}{\partial y_i}\right] = \frac{\partial D(\mathbf{y})}{\partial y_j}, \quad (13)$$

in the domain of a single periodic unit, with periodic boundary conditions (cf. their equation, reference 22, Eq. 2.17, p. 15). This equation for χ^j is a steady-state equation even for time-dependent diffusion, as is shown by Bensoussan et al., given the assumption that ϵ is small. The second term on the left-hand side of Eq. 12, involving r, is the homogenized reaction term, and it is clear that it is decoupled from the first (diffusion) term. This homogenized equation is the leading behavior as $\epsilon \to 0$; further corrections in ϵ are given by Bensoussan et al., but their use is not justified here because of the limited precision of any experimental data available for comparison. From the homogenized Eq. 12, it is clear that the effective diffusivity is

$$D_{ij}^{\text{eff}} = \frac{1}{V}\int_P \left(D(\mathbf{y})\delta_{ij} - D(\mathbf{y})\frac{\partial\chi^j}{\partial y_i}\right)d\mathbf{y}. \quad (14)$$

Once the effective diffusivity is determined, the concentration profile in a tissue region can be determined from the simpler equation

$$\frac{\partial\langle c\rangle}{\partial t} - D_{\text{eff}}^{ij}\frac{\partial^2\langle c\rangle}{\partial x_i \partial x_j} = r_{\text{eff}}(\langle c\rangle), \quad (15)$$

where r_{eff} is the effective reaction rate, which turns out to be the simple average

$$r_{\text{eff}}(\langle c\rangle) = \frac{1}{V}\int_P r(\langle c\rangle, \mathbf{y})\,d\mathbf{y}. \quad (16)$$

The diffusivity tensor D_{eff}^{ij} can be shown to be symmetric, but it is not necessarily diagonal. For the cell arrangements shown in Fig. 1, we make the obvious choice of x_1, x_2, and x_3 directions as perpendicular to faces of the cells. Then, by symmetry, the effective diffusivity is diagonal:

$$\frac{\partial\langle c\rangle}{\partial t} = D_{\text{eff}}^{11}\frac{\partial^2\langle c\rangle}{\partial x_1^2} + D_{\text{eff}}^{22}\frac{\partial^2\langle c\rangle}{\partial x_2^2} + D_{\text{eff}}^{33}\frac{\partial^2\langle c\rangle}{\partial x_3^2}; \quad (17)$$

(henceforth, the reaction terms are omitted, since this paper is concerned with the diffusivity.) Although the interstitium is isotropic, when the size or arrangement of cells is different in different directions, the effective diffusivity may not be the same in all directions. That is, the

constants D_{eff}^{11}, D_{eff}^{22}, and D_{eff}^{33} are not all equal in the staggered and elongated cases.

The equation for χ can be simplified by noting that since $D(\mathbf{y}) = 0$ inside the cells and $D(\mathbf{y}) = D_{\text{int}}$ in the interstitium, from Eq. 13, $\chi = 0$ inside the cells, and in the interstitium χ satisfies Laplace's equation

$$\frac{\partial^2 \chi}{\partial y_1^2} + \frac{\partial^2 \chi}{\partial y_2^2} + \frac{\partial^2 \chi}{\partial y_3^2} = 0. \tag{18}$$

The periodic boundary conditions on χ on the boundary of the periodic unit P have already been noted. It remains only to deduce the boundary conditions on χ at the cell surfaces. As already mentioned, the cell surfaces are all planar and oriented in one of the three Cartesian directions. Consider any such surface, which is on the plane $y_i = A$. Integrate Eq. 13 from $y_i = A^-$ (assumed to be inside the cell) to $y_i = A^+$ (assumed to be outside the cell). The result is

$$D(\mathbf{y}) \left.\frac{\partial \chi^j}{\partial y_i}\right|_{y_i = A^+} - D(\mathbf{y}) \left.\frac{\partial \chi^j}{\partial y_i}\right|_{y_i = A^-} = [D(\mathbf{y})|_{A^+} - D(\mathbf{y})|_{A^-}]\delta_{ij}, \tag{19}$$

which simplifies to

$$\left.\frac{\partial \chi^j}{\partial y_i}\right|_{y_i = A^+} = \delta_{ij}. \tag{20}$$

This is the boundary condition to be used on χ^j, which now only has to be solved for in the interstitial region. It is easy to show that when $y_i = A^-$ is outside the cell and $y_i = A^+$ is inside,

$$\left.\frac{\partial \chi^j}{\partial y_i}\right|_{y_i = A^-} = \delta_{ij}. \tag{21}$$

It is clear that the boundary conditions for χ^j on the cell surface generalize to

$$\mathbf{n} \cdot \nabla c = \mathbf{n} \cdot \mathbf{e}_j. \tag{22}$$

An equation and boundary conditions analogous to the ones for χ^j obtained above were derived by Blum et al. (24) for a periodic lattice of interconnected beams rather than cuboidal cells. Since their derivation is elaborate, it is interesting to note that this system follows very simply from homogenization theory.

The Eq. 18 with periodic boundary conditions on the periodic unit faces, and the above-described boundary conditions (Eq. 22) on the cell surfaces, is solved numerically by setting up an evenly-spaced cubic array of grid points throughout the domain (that is, the interstitial space), and using the relaxation method (reference 25, pp. 307–312). At each iteration, the value of χ at each grid point in the interior is replaced by the average of its nearest neighbors; this converges to a solution of the diffusion equation. By symmetry the domain of solution is reduced from an entire periodic unit to either an eighth or a quarter of a periodic unit. The interstitial spaces are always 20 grid points wide. Since gradients are highest across the interstitial spaces, rather than along them, interstitial volume fraction is decreased by increasing the cell side lengths from about 50 to about 200 grid points, rather than decreasing the number of grid points across the interstitium. Convergence was assumed when the calculated effective diffusivity changed by less than 0.001% in one iteration.

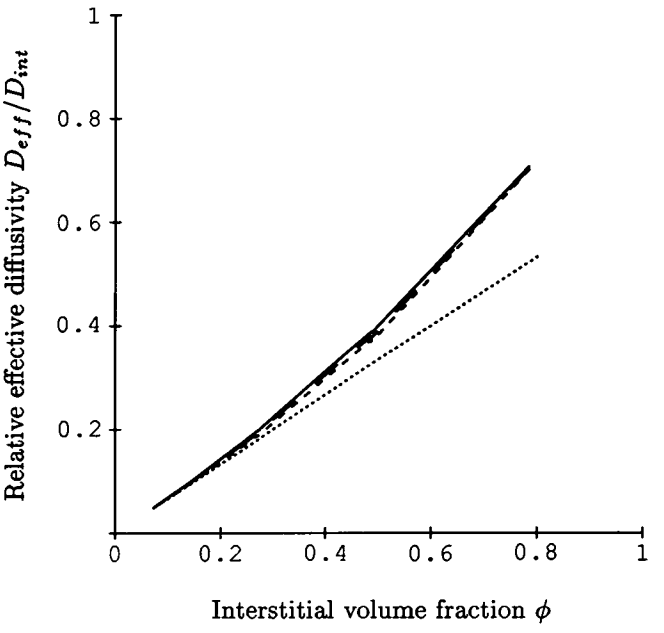

FIGURE 3 Effective diffusivity as a function of interstitial volume fraction: comparison of aligned, staggered, and doubly staggered cases. Solid curve: aligned; long dashes: staggered in one direction; short dashes: staggered in two directions; dotted line: $D_{\text{eff}}/D_{\text{int}} = (^2/_3)\phi$ approximation for small ϕ (aligned).

RESULTS AND DISCUSSION

A molecule diffusing past staggered cells must zigzag along a pathway longer than that of a molecule moving down straight channels between aligned cells, so staggering should decrease the effective diffusivity D_{eff}. Fig. 3 shows plots of the ratio $D_{\text{eff}}/D_{\text{int}}$ for values of ϕ in the physiological range, for cubic cells aligned, staggered in one direction, and staggered in two directions. In the case of aligned cells, the diffusivity is, of course, the same in all directions. In the staggered cases, the diffusivities plotted are for diffusion in the direction where the pathways zigzag the most. While the effective diffusivity is slightly smaller for the staggered cases, the effect of staggering is remarkably small. Fig. 3 strongly suggests that as long as cells are roughly cuboidal, that is, not very elongated, how they are arranged is relatively unimportant; the key factor of the geometry is the volume fraction available for diffusion. The curve $2\phi/(3-\phi)$, repre-

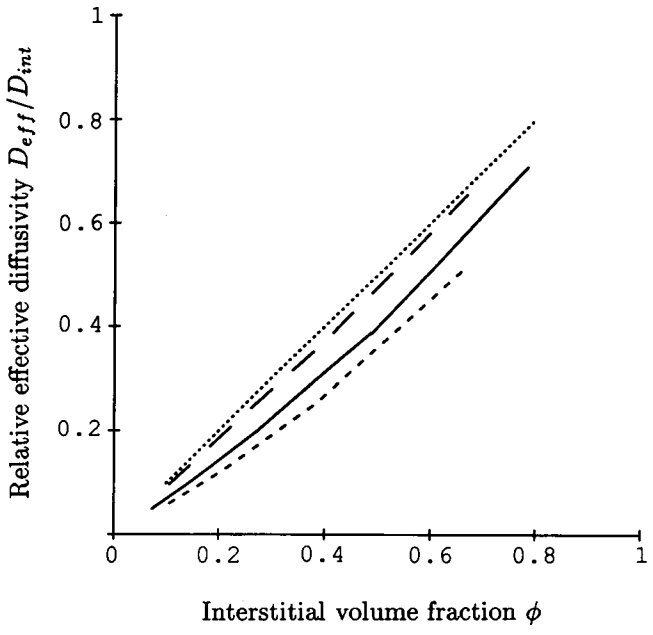

FIGURE 4 Effect of elongating (aligned) cells on effective diffusivity. Solid curve: cubic cells (1:1:1); long dashes: cells elongated (5:1:1) in direction of diffusion; short dashes: cells elongated (1:5:1) perpendicular to direction of diffusion; dotted line: upper bound $D_{eff}/D_{int} = \phi$.

senting Milton's upper bound for the isotropic case, is very close to all three computed curves shown in Fig. 3. Since staggering the cells has so little effect, we conjecture that this is a good approximation for most actual (unelongated) cell arrangements.

In Fig. 4, the effect of cell elongation in one direction is shown. As discussed earlier, elongating the cells increases the effective diffusivity in the direction of elongation. Fig. 4 shows that the effective diffusivity past spindle-shaped cells is not very different from D_{eff} for aligned cells.

There remains the issue of whether the assumption of cuboidal-shaped cells has a significant effect on the results, since actual cells are irregularly shaped. If the interstitial volume fraction is held fixed, going from cuboidal to irregular shapes could have several effects. Firstly, depending on how the irregular shapes were arranged, there could be the analog of staggering for cuboidal cells. We have seen that the effect of staggering is slight. This suggests that a random, rather than ordered, arrangement would have little effect, except that the interstitial volume fraction could not be made as low. Secondly, irregularly shaped cells would cause the width of the interstitial channels to vary. In our cuboidal cell model, the width of the channels is constant. However, it was shown above that the effective diffusivity is not very sensitive to variations in channel width. This argument was based on a two-dimensional geometry, corresponding to long ridge-like constrictions in three dimensions. In reality, constrictions are likely to be more localized, resulting in even less reduction in effective diffusivity. For instance, a constriction localized near a point is easily bypassed because of the presence of many parallel pathways for diffusion in three dimensions. Available data do not suggest the existence of ridge-like constrictions in the interstitial spaces of tumors. Thirdly, the cells might be shaped so as to make the channel midplane undergo many changes of direction, not just on a cellular length scale (which is the staggering effect) but on sub-cellular length scales. Photographs of tissue slices do not generally suggest this; most cell membranes do not have extensive irregularities on sub-cellular length scales (there are certain exceptions such as intestinal villi, which, in accordance with their function, have many indentations). These considerations suggest that the choice of ordered arrangements of cuboidal-shaped cells, as opposed to other *regular* shapes such as spherical or cylindrical, in either ordered or random arrangement, had little effect on our results.

With the above results, it is possible to estimate the relative importance of volume exclusion effects and interstitial structure. While some data exist for interstitial volume fractions in tumor tissue (9), and some data for (effective) diffusivities of monoclonal antibodies in tumors in vivo (15) and tumor spheroids in vitro (2), there do not seem to be any available data with both quantities measured simultaneously in the same tissue. For typical tumors, the interstitial volume fraction ϕ is in the range 25–50% (15). For this range, our model predicts values of D_{eff}/D_{int} in the range 0.19–0.40. Comparing this with the experimental value $D_{eff}/D_{aq} = 0.022$, from (15), for fluorescein isothiocyanate-conjugated nonspecific polyclonal rabbit IgG in VX2 carcinoma in a rabbit-ear chamber implies that D_{int}/D_{aq} is in the range 0.05–0.12. That is, the interstitial structure alone reduces the diffusivity by about an order of magnitude relative to the diffusivity in water.

CONCLUSIONS

Our main conclusions are summarized as follows:

(1) The shape and arrangement of cells have little effect on the effective diffusivity, for a given interstitial volume fraction.

(2) The effective diffusivity D_{eff} is determined mainly by the volume fraction ϕ. A rough estimate is

$$\frac{2}{3}\phi \le \frac{D_{eff}}{D_{int}} \le \phi, \tag{23}$$

and a good approximation for unelongated cells is

$$\frac{D_{eff}}{D_{int}} \approx \frac{2\phi}{3-\phi}. \tag{24}$$

(3) Our calculations of the volume exclusion effect, combined with data from the literature, suggest that the

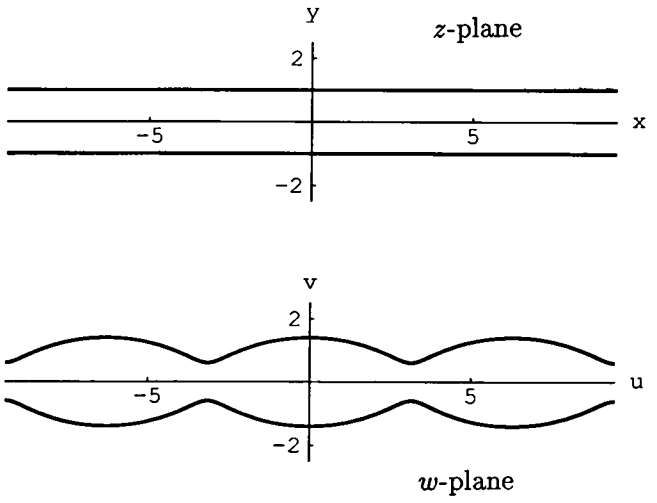

FIGURE 5 The conformal mapping $\omega(z) = z + b \sin z/\sinh a$, for $a = 1$, $b = 0.4$, maps an infinite straight strip in the $z = x + iy$ plane to an infinite variable-width strip in the $\omega = u + iv$ plane.

diffusivity of a monoclonal antibody in the interstitium is one-tenth to one-twentieth its diffusivity in water.

(4) For small interstitial spaces ($\approx$20%), volume exclusion has as much effect as interstitial structure on the effective diffusivity in tissue.

(5) Since volume exclusion is independent of molecular weight, using antibody fragments instead of whole antibody will not reduce diffusion time scales as much as might be expected, especially if interstitial spaces are small.

APPENDIX

The long-wavelength (one-dimensional) approximation given in reference 7 always overestimates the flux in a variable-width channel. To investigate more accurately the effect of variable-width, when the wavelength of the variation is not very large, we consider *two*-dimensional diffusion in a channel of variable width, and compare it to diffusion in a constant-width channel of the same average width. This is done by considering the conformal mapping

$$\omega(z) = z + \frac{b}{\sinh(a)} \sin(\omega z), \tag{25}$$

which maps the infinite constant-width strip $-\infty < x < \infty$, $-a < y < a$ in the (x, y)-plane to an infinite variable-width strip in the (u, v)-plane. The boundaries of this wavy strip are given parametrically by

$$(u(s), v(s)) = (s + b \coth(\omega a) \sin(\omega s), \pm(a + b \cos(\omega s))), \tag{26}$$

as shown in Fig. 5. For given imposed concentrations at, say, x or $u = 0$ and x or $u = 2N\pi/\omega$ (N any integer) and no flux through the channel walls, these two channels have the same flux. This follows from the fact that solutions of Laplace's equation remain solutions when the domain is conformally mapped. The average width of the wavy channel is $2a + \omega b^2 \coth(\omega a)$. The ratio of the flux in the wavy channel to the flux in a straight channel of the same average width is

$$\frac{(\text{Flux})_{\text{wavy}}}{(\text{Flux})_{\text{straight}}} = \frac{1}{1 + \dfrac{\omega b^2}{2a} \coth(\omega a)}. \tag{27}$$

The wavelength of the variation is $2\pi/\omega$, and b/a is approximately the ratio of width variation to average width. In the case $\omega a = 1$ and $b/a = 0.5$, the ratio of wavelength to average width is 2.7 and the flux ratio in (27) is 0.86. When $\omega a = 3$ and $b/a = 0.3$, the wavelength is 0.92 times the average width and the ratio in (27) is 0.88. We conclude that variations in channel width have only a small effect on effective diffusivity, except for variations of large amplitude (much greater than half the average width) or high frequency (wavelength much greater than average width). For most cell types, observations do not suggest such extreme variations.

This work was supported by the National Institutes of Health under grants HL-17421, HL-07249, and CA-40355.

Received for publication 20 May 1992 and in final form 27 January 1993.

REFERENCES

1. Jain, R. K. 1989. Delivery of novel therapeutic agents in tumors: physiological barriers and strategies. *J. Natl. Cancer Inst.* 81:570–576.
2. McFadden, R., and C. S. Kwok. 1988. Mathematical model of simultaneous diffusion and binding of antitumor antibodies in multicellular human tumor spheroids. *Cancer Res.* 48:4032–4037.
3. Chary, S. R., and R. K. Jain. 1989. Direct measurement of interstitial convection and diffusion of albumin in normal and neoplastic tissues by fluorescence photobleaching. *Proc. Natl. Acad. Sci. USA.* 86:5385–5389.
4. Levick, J. R. 1987. Flow through interstitium and other fibrous matrices. *Quart. J. Exp. Physiol.* 72:409–438.
5. Landis, E. M., and J. R. Pappenheimer. 1963. Exchange of substances through the capillary walls. *In* Handbook of Physiology, Section 2. Circulation, Vol. II, W. F. Hamilton and P. Dow, editors. American Physiological Society, Washington, DC. 961–1034.
6. Torquato, S. 1987. Thermal conductivity of disordered heterogeneous media from the microstructure. *Revs. Chem. Eng.* 4:151–204.
7. Torquato, S. 1991. Random heterogeneous media: microstructure and improved bounds on effective properties. *Appl. Mech. Rev.* 44:37–76.
8. Happel, J., and H. Brenner. 1973. Low-Reynolds-Number Hydrodynamics. Noordhoff-Sijthoff, Leyden. 553 pp.
9. Jain, R. K. 1987. Transport of molecules in the tumor interstitium: a review. *Cancer Res.* 47:3039–3051.
10. De Santes, K., D. Slamon, S. K. Anderson, M. Shepard, B. Fendly, D. Maneval, and O. Press. 1992. Radiolabelled antibody targeting of the HER-2/neu oncoprotein. *Cancer Res.* 52:1916–1923.
11. Pavelic, Z. P., L. Pavelic, E. E. Lower, M. Gapany, S. Gapany, E. A. Barker, and H. D. Preisler. 1992. c-myc, c-erbB-2, and Ki-67 expression in normal breast tissue and in invasive and noninvasive breast carcinoma. *Cancer Res.* 52:2597–2602.
12. Kelvin, Lord. 1887. On the division of space with minimum partitional area. *Phil. Mag.* 24:503–514.
13. Matzke, E. B. 1946. The three-dimensional shape of bubbles in foam—an analysis of the role of surface forces in three-dimensional cell shape determination. *Am. J. Bot.* 33:58–80.

14. Kittrell, F. S., C. Oborn, and D. Medina. 1992. Development of mammary preneoplasias in vivo from mouse mammary epithelial cell lines in vitro. *Cancer Res.* 52:1924–1932.

15. Clauss, M. A., and R. K. Jain. 1990. Interstitial transport of rabbit and sheep antibodies in normal and neoplastic tissues. *Cancer Res.* 50:3487–92.

16. Vaughan, A. T. M., P. Anderson, P. W. Dykes, C. E. Chapman, and A. R. Bradwell. 1987. Limitations to the killing of tumours using radiolabelled antibodies. *Br. J. Radiology.* 60:567–578.

17. Bear, J. 1969. Hydrodynamic dispersion. *In* Flow through Porous Media. R. J. M. de Weist, editor. Academic Press, New York. 109–199.

18. Schultz, J. S., and W. Armstrong. 1978. Permeability of interstitial space of muscle (rat diaphragm) to solutes of different molecular weights. *J. Pharm. Sci.* 67:696–700.

19. Nicholson, C., and J. M. Phillips. 1981. Ion diffusion modified by tortuosity and volume fraction in the extracellular microenvironment of the rat cerebellum. *J. Physiol.* 321:225–257.

20. Milton, G. W. 1980. Bounds on the complex dielectric constant of a composite material. *Appl. Phys. Lett.* 37:300–302.

21. Garabedian, P. R. 1986. Partial Differential Equations. Chelsea House Educational Publishers, New York. 672 pp.

22. Bensoussan, A., J. L. Lions, and G. Papanicolaou. 1978. Asymptotic Analysis for Periodic Structures. North Holland Science Publishers, New York. 700 pp.

23. Buchsbaum, D. J., R. L. Wahl, S. D. Glenn, D. P. Normolle, and M. S. Kaminski. 1992. Improved delivery of radiolabelled anti-B1 monoclonal antibody to Raji lymphoma xenografts by predosing with unlabeled anti-B1 monoclonal antibody. *Cancer Res.* 52:637–642.

24. Blum, J. J., G. Lawler, M. Reed, and I. Shin. 1989. Effect of cytoskeletal geometry on intracellular diffusion. *Biophys. J.* 56:995–1005.

25. Jeffreys, H., and B. S. Jeffreys. 1956. Methods of Mathematical Physics, 3rd. Ed. Cambridge University Press, Cambridge, UK. 714 pp.